
**Liquid Crystals**
Publication details, including instructions for authors and subscription information:
http://www.informaworld.com/smpp/title~content=t713926090

# Structure of planar solitons in nematic and smectic liquid crystals

N. Andal[a]; G. S. Ranganath[a]
[a] Raman Research Institute, Bangalore, India

**To cite this Article** Andal, N. and Ranganath, G. S.(1996) 'Structure of planar solitons in nematic and smectic liquid crystals', Liquid Crystals, 20: 3, 321 — 330
**To link to this Article: DOI:** 10.1080/02678299608032041
**URL:** http://dx.doi.org/10.1080/02678299608032041

LIQUID CRYSTALS, 1996, VOL. 20, No. 3, 321–330

# Structure of planar solitons in nematic and smectic liquid crystals

by N. ANDAL and G. S. RANGANATH*
Raman Research Institute, Bangalore-560080, India

*(Received 6 September 1995; accepted 6 October 1995)*

We have undertaken a theoretical study on the structure of planar solitons in nematic and smectic liquid crystals. In nematics we find a soliton solution which can be looked upon as an intertwine between two solitons. In a nematic obtained by unwinding a cholesteric and in a nematic with very high dielectric anisotropy, we have worked out energetics of solitons. A $2\pi$ soliton in a ferronematic or a smectic C becomes unstable due to the splay bend elastic anisotropy. The structures of $\pi$ solitons in smectic A and smectic C in the neighbourhood of a $S_A$–$S_C$ phase transition have also been studied.



## 1. Introduction

In an external electric or magnetic field a liquid crystal can adopt a non-singular static director configuration such that most of the distortion in the director field is confined to a narrow region of space and is stabilized by the field. In far off regions the director is in the uniform state. In spite of its infinite extent it has a finite energy of distortion. Such structures have been termed as solitons in liquid crystal literature [1, 2]. However this is different from 'true' solitons which are traveling solitary waves and which retain their shape and structure after pairwise collision. In our paper the term soliton will refer to static structures only. In a planar soliton the distortion is confined to a wall. Hence it is also referred to as a wall. Helfrich walls [3] are good examples of this state.

A lot of effort has gone into finding new planar soliton states in liquid crystals, in view of their importance in phase transitions and structural instabilities [4–9]. However in all these studies attention has not been paid to the following specific situations.

- Effects of elastic anisotropy on the energetics of planar solitons that can exist in a nematic obtained from magnetic (or electric) unwinding of a cholesteric liquid crystal.
- The explicit effects of flexo-electricity and elastic anisotropy on the energetics of these topological objects in nematics in an electric field.
- Effects of non-planar distortions on planar solitons.
- Evolution of a $2\pi$ soliton structure in smectics and ferronematics after the onset of instability.

We address ourselves to these specific situations in this paper. In addition we have also commented upon the structure of $\pi$ solitons near a smectic A ($S_A$)–smectic C ($S_C$) phase transition.

In nematics with negative diamagnetic anisotropy we find an out of plane distortion of a planar soliton to lead to new types of solitons. In particular they are in the nature of combination of two solitons. We call such structures *intertwined solitons*. In a nematic state obtained by magnetically or electrically unwinding a cholesteric, we find a range of fields over which it is possible for a bend soliton to be energetically favourable compared to an anti-twist soliton whose twist is opposite in sense to that of the parent cholesteric. In nematics, in an electric field, with very high dielectric anisotropy a flexo electric lattice does not form spontaneously [10, 11]. In such nematics, we find a twist soliton to be of lower energy compared to the flexo-electrically stable bend soliton. We next work out field and elastic anisotropy induced instabilities that occur in a $2\pi$ splay or bend soliton in a ferronematic (FN) or a smectic C ($S_C$). We have also considered the structure of $\pi$ planar solitons in the neighbourhood of smectic A ($S_A$) and smectic C ($S_C$) transitions. In this problem attention has been paid to the order parameter variations associated with solitons.

## 2. Intertwined solitons

In nematics with negative diamagnetic anisotropy ($\chi_a < 0$), in a magnetic field **H**, a topologically permitted non-singular solution is a cylindrically symmetric structure such that at $r = \infty$, the director **n** is perpendicular to **H** and is along **H** at $r = 0$. It may be mentioned that **n** can be either in an all radial or all circular state at $r = \infty$. Figure 1 (*a*) shows an all radial structure. We can also construct planar solitons in such nematics. In a planar soliton the director **n** is confined to a plane [2] and its distortions are predominantly within a wall. There are three possible planar solitons. These are

*Author for correspondence.

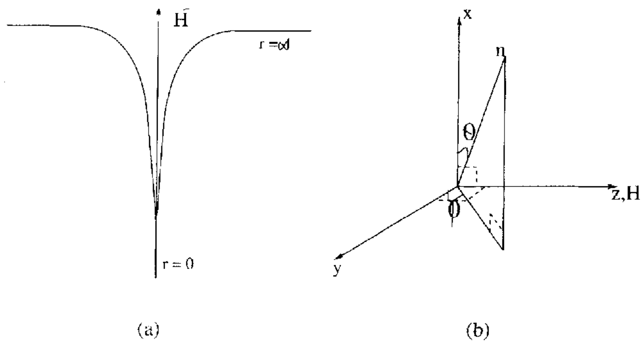


Figure 1. (*a*) All radial splay–bend soliton. (*b*) The coordinate system with reference to which the planar solitons are described.

similar to planar solitons of $\chi_a > 0$ materials which have been studied extensively both theoretically and experimentally [5–8]. Here we refer **n** and **H** to a coordinate system shown in figure 1 (*b*).

Firstly we consider the bend soliton. The director is perpendicular to the $z$ axis at $z = \pm\infty$ and $n_x = 0$ everywhere. These states are of minimum energy since $\chi_a < 0$ and they can be connected by a continuous bend in the director in the $y$–$z$ plane. The free energy density is given by

$$F = \frac{K}{2}[(\nabla\cdot\mathbf{n})^2 + (\nabla\times\mathbf{n})^2] - \frac{\chi_a}{2}(\mathbf{H}\cdot\mathbf{n})^2. \qquad (1)$$

Here $K$ is the elastic constant in the one constant approximation. Minimization of the total energy gives

$$\Phi_{zz} = \frac{\chi_a H^2}{K}\sin\phi\cos\phi \qquad (2)$$

where $\phi_{zz} = \partial^2\phi/\partial z^2$. This permits a solution described by $n_x = 0$, $n_y = \cos\phi$ and $n_z = \sin\phi$ with

$$\phi = 2\tan^{-1}\left(\exp\left[\frac{z}{\eta}\right]\right) \quad \text{and} \quad \theta = \pi/2 \qquad (3)$$

where $\eta = (K/\chi_a H^2)^{1/2}$. It is shown in figure 2 (*a*). This is a bend soliton.

If instead, we consider $\phi$ to vary along $x$ with $\phi = 0$ at $x = -\infty$ and $\phi = \pi$ at $x = +\infty$ and $n_x = 0$ everywhere, we get a twist soliton. This is shown in figure 2 (*b*). It is described by

$$\phi = 2\tan^{-1}\left(\exp\left[\frac{x}{\eta}\right]\right) \quad \text{and} \quad \theta = \pi/2 \qquad (4)$$

Finally we can also construct a splay soliton by considering $\phi = 0$ at $y = -\infty$ and $\phi = \pi$ at $y = +\infty$ with $n_x = 0$ everywhere. Here the variations in $\phi$ are along the $y$ axis. This is shown in figure 2 (*c*). This structure is described by

$$\phi = 2\tan^{-1}\left(\exp\left[\frac{y}{\eta}\right]\right) \quad \text{and} \quad \theta = \pi/2. \qquad (5)$$

We now consider out of plane distortions in these planar solitons i.e. $n_x = \cos\theta$, $n_y = \sin\theta\cos\phi$ and $n_z =$

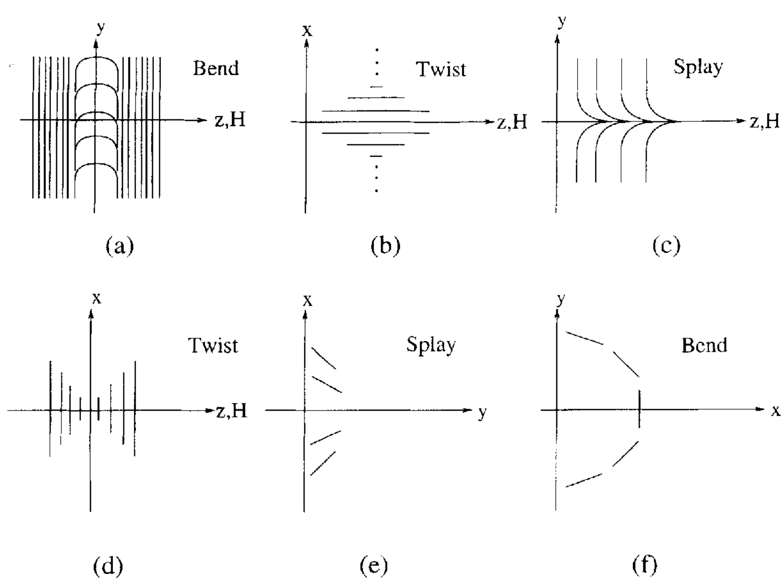


Figure 2. π planar solitions (*a*) bend (*b*) twist and (*c*) splay. Figures (*d*), (*e*) and (*f*) refer to the arbitrary out of plane $\theta$ deformations that go, respectively, with the bend, twist and splay solitons.

$\sin\theta \sin\phi$. The free energy density is given by

$$F = \frac{K}{2}[(\nabla\theta)^2 + (\sin\theta)^2((\nabla\phi)^2 - E_2(\sin\phi)^2)]. \quad (6)$$

Here $E_2 = \chi_a H^2/K$. We consider materials with $\chi_a < 0$, i.e. with negatiave diamagnetic anisotropy. The equations of equilibrium are

$$\nabla^2\theta = \sin\theta\cos\theta[(\nabla\phi)^2 - E_2(\sin\phi)^2] \quad (7)$$

and

$$\nabla^2\phi = -E_2\sin\phi\cos\phi - \cot\theta[2(\nabla\theta.\nabla\phi)]. \quad (8)$$

We first deal with the case where $\theta$ and $\phi$ vary along $z$. Let us consider a director orientation with $\phi = 0$, $\theta = \theta_1$ at $z = -\infty$ and $\phi = 0$, $\theta = \theta_2$ at $z = +\infty$. These director states are of minimum energy for a field along $z$ axis since $\chi_a$ is negative. They can be connected by a uniform twist of $\Delta\theta = (\theta_2 - \theta_1)$ about $z$. This is shown in figure 2 (*d*). Since this confines the director everywhere to a plane perpendicular to the field, its elastic distortion is not coupled to the field. Hence left to itself it will unwind on its own and go to the uniform state. But interestingly in view of (7) and (8) we find that this twist in $\theta$ can be coupled to the field through variations in $\phi$. Solving these equations numerically yield $\theta$ and $\phi$ variations as shown in figures 3 (*a*) to (*d*). We find that a $\pi$ bend soliton described by variations in $\phi$ alone is intertwined with a $\Delta\theta$ twist soliton described by variations in $\theta$ alone. The value of the net twist $\Delta\theta$, can be made to change continuously from 0 to $\pi$. In figure 3 (*d*) we see that a $\pi$ bend soliton is coupled with a $\pi$ twist soliton. The twist per unit length (as given by the slope at the centre) in the $\Delta\theta$ soliton is seen to increase with increasing $\Delta\theta$.

Instead of $\phi$ and $\theta$ variations along $z$ we could have considered their variations along $x$. In this case the $\phi$ distortion represents a twist configuration (see figure 2 (*b*)) and $\theta$ distortion represents a splay in the director field as shown in figure 2 (*e*). Hence in this case a $\Delta\theta$ splay soliton is intertwined with a $\pi$ twist soliton.

In the same way variations of $\phi$ and $\theta$ along $y$ axis lead to splay and bend distortions as shown respectively in figure 2 (*c*) and figure 2 (*f*). In this case a $\Delta\theta$ bend soliton is intertwined with a $\pi$ splay soliton.

Interestingly we find such intertwined soliton states only for $\chi_a < 0$ nematics. We can easily understand this because a $\theta$ distortion in the $\chi_a > 0$ nematics leads to an increase in the magnetic energy.

### 3. Nematics with a latent lattice symmetry

In this section we study the effect of a latent lattice symmetry on planar solitons in nematics. The soliton itself is produced by the dielectric or diamagnetic interactions with the field. It is very well known [12, 13] that in a magnetic field applied perpendicular to the twist axis and above a threshold $H_c$ a cholesteric becomes a nematic. We call this a nematic with a latent lattice. The free energy density of this system is

$$F = \frac{K_{22}}{2}(\phi_z - q_0)^2 + \frac{1}{2}\chi_a H^2(\sin\phi)^2 - \frac{K_{22}}{2}q_0^2. \quad (9)$$

Here $\phi_z = \partial\phi/\partial z$, $q_0 = 2\pi/P$, with $P$ as the pitch and $K_{22}$ is the twist elastic constant. This leads to an equation of equilibrium identical to (2) which permits a $\pi$-twist and $\pi$-anti-twist soliton described respectively by

$$\phi = 2\tan^{-1}\left[\exp\left(\frac{\pm z}{\xi}\right)\right] \quad (10)$$

with

$$\xi = \left(\frac{K_{22}}{\chi_a H^2}\right)^{1/2}. \quad (11)$$

A twist soliton (TS) has the same sense of twist as the parent cholesteric while the anti-twist soliton (ATS) has an opposite sense of twist. The total distortion energies of these solitons are given by

$$E_{ATS} = K_{22}[(2/\xi) + q_0\pi]$$

and

$$E_{TS} = K_{22}[(2/\xi) - q_0\pi].$$

For $(\pi/2)q_0\xi > 1$ i.e. for $H < (\pi/2)q_0(K_{22}/\chi_a)^{1/2}$, the energy $E_{TS}$ of a twist soliton becomes negative indicating a spontaneous generation of such twist solitons leading to a soliton lattice. However for $(\pi/2)q_0\xi < 1$, we have the undistorted nematic to be of the lowest energy with the ATS having a higher energy compared to the TS. An interesting possibility exists in a $\chi_a > 0$ material where a bend soliton can connect the same base states as that associated with an ATS. These features are shown in figure 4. This bend soliton can become energetically favourable compared to an ATS. For this to happen the net energy of the bend soliton should be lower than that of the ATS which leads to the condition

$$\left(\frac{\bar{K}}{K_{22}}\right)^{1/2} - 1 < \frac{\pi}{2}q_0\xi \quad (12)$$

where $\bar{K}$ is the bend or splay elastic constant. This together with the condition $(\pi/2)q_0\xi < 1$ for the nematic state leads to

$$\left(\frac{\bar{K}}{K_{22}}\right)^{1/2} - 1 < \frac{\pi}{2}q_0\xi < 1. \quad (13)$$

Hence for $\bar{K} < 4K_{22}$ a bend soliton is favourable compared to an ATS. However in a given situation this occurs only upto a field $H'$ above $H_C$. At $H'$ the inequality (12) is just violated. For $H > H'$, the ATS is favoured energetically. However, in the one constant approximation, in such a nematic a bend soliton is

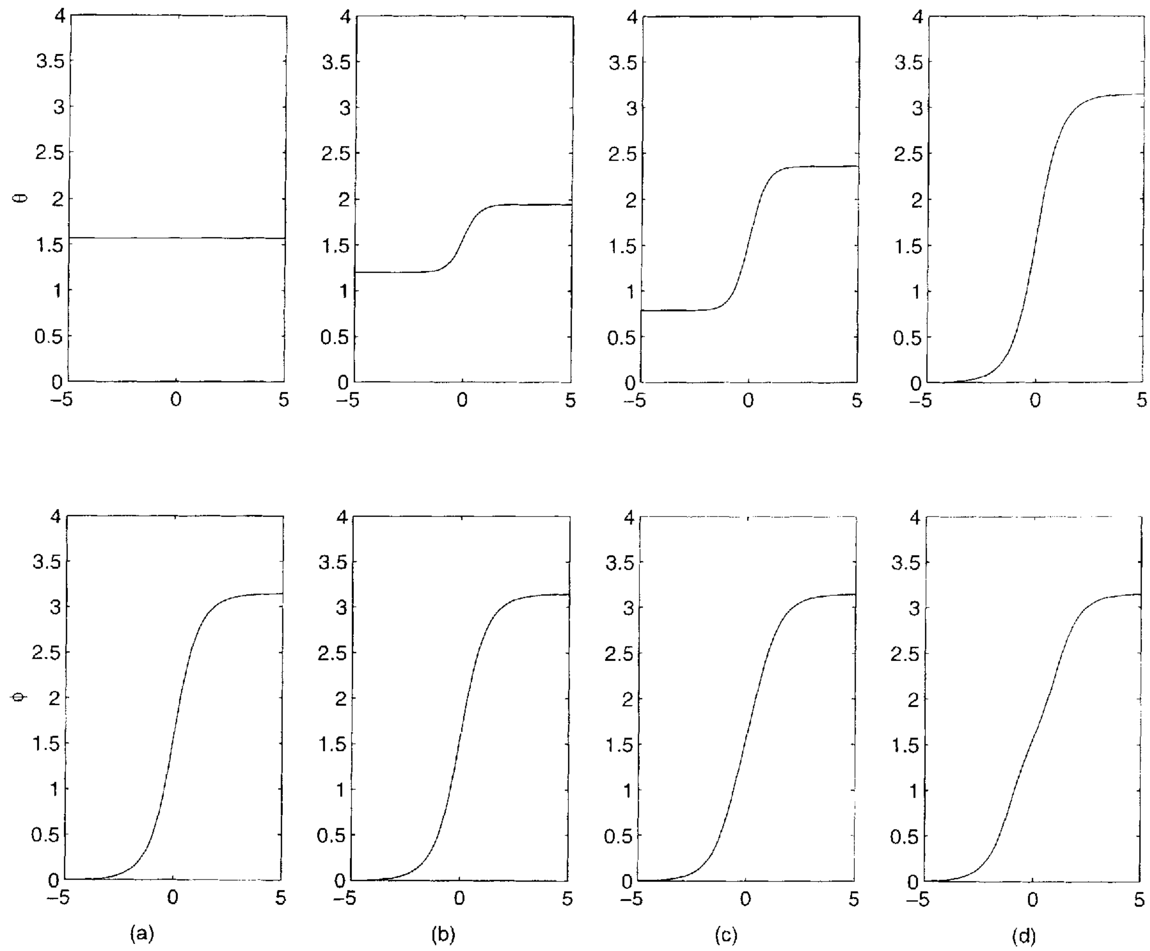


Figure 3. The $\theta$ and $\phi$ profiles associated with an intertwined soliton. The abscissa is in units of $z/\xi$ [$E_2 = 10^6$].

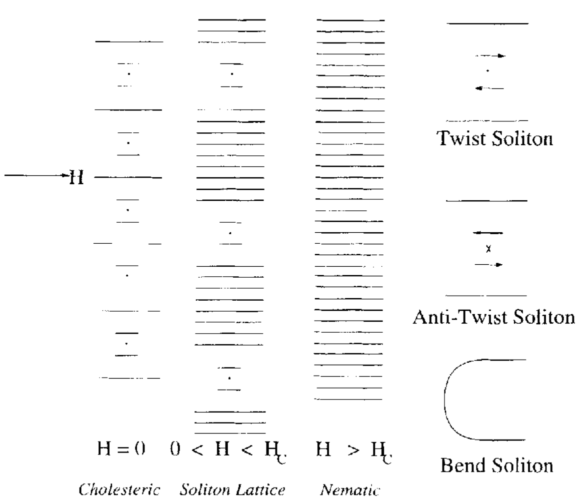


Figure 4. Construction of twist, anti-twist and bend solitons in a nematic obtained by unwinding a $\chi_a > 0$ cholesteric. We also show in the figure the process of cholesteric unwinding through the formation of a soliton lattice. Arrow heads have been used to distinguish a twist from an anti-twist.

always favoured over an ATS. It may be mentioned that in a normal nematic a bend soliton always has a higher energy than the TS or ATS since $K_{22} < \bar{K}$.

We now consider flexo-electric effects in a nematic with positive dielectric anisotropy $\varepsilon_a$. For such materials if $|\varepsilon_a| > \pi^3 e^{*2}/4\bar{K}$ where $e^* = e_1 - e_3$, with $e_1$ and $e_3$ as flexoelectric coefficients, it is well known that a spontaneous splay–bend flexo-electric lattice is not possible [10, 11]. In such nematics we can construct bend solitons of opposite bends. These have their flexo-electric polarization either along or opposite to the external electric field. We consider the bend soliton of lower energy. Its flexo polarization is along the external field. In view of the above analysis we can again consider a twist soliton or an anti-twist soliton in the very same geometry. These twist solitons are equally energetic. In this case, for the twist state or anti-twist state to be more favourable than the bend soliton considered, we have to satisfy the inequality

$$\frac{\pi}{2} e^* \left(\frac{\pi}{\bar{K}\varepsilon_a}\right)^{1/2} < \left[1 - \left(\frac{K_{22}}{\bar{K}}\right)^{1/2}\right]. \qquad (14)$$

Since $K_{22}$ is invariably less than $\bar{K}$ this inequality is sufficient leading to an interesting conclusion that a twist soliton is preferred to the energetically permitted bend soliton.

In a nematic obtained by unwinding a cholesteric in an electric field, we find a totally different answer. In this case, there should be no spontaneous twist, splay or bend. Hence, here a flexo-electrically permitted bend soliton can be made energetically favourable compared to an ATS by satisfying two inequalities.

$$\left(\frac{\bar{K}}{K_{22}}\right)^{1/2} - 1 < \frac{\pi q_0}{2}\left(\frac{4\pi K_{22}}{\varepsilon_a E^2}\right)^{1/2} < 1 \qquad (15)$$

and

$$\frac{\pi e^*}{2}\left(\frac{\pi}{\bar{K}\varepsilon_a}\right)^{1/2} < 1. \qquad (16)$$

For values of $\varepsilon_a$ satisfying (16), the inequality (15) will be satisfied only in the range of fields $E_c < E < E'$ as in the case of cholesterics. Only then a bend soliton is favoured in such a nematic with a very large $\varepsilon_a$.

It may be mentioned that in $\varepsilon_a$ or $\chi_a$ negative nematics it is not possible to have both bend and twist soliton as solutions with the same base states, in a magnetic or an electric field alone. However in crossed electric and magnetic fields, it is possible to stabilize a bend soliton or a twist soliton between the same base states. Since their energies can be independently varied by altering the strengths of the fields, it is possible to have the energy of the bend soliton to be less than the energy of an anti-twist soliton.

In conclusion, unlike the usual nematics, in these nematics which have a latent lattice symmetry we find some new results.

## 4. Stability of a $2\pi$ soliton

We consider in this section the stability of a $2\pi$ planar soliton state. Here inside the wall the director is confined to a plane and it turns through $2\pi$. That field induces instabilities in a $2\pi$ twist soliton has already been pointed out by earlier investigators [14, 15]. Here we address ourselves to $2\pi$ splay or bend solitons.

### 4.1. *Effects of field*

In smectic C ($S_C$), in addition to the molecular tilt angle $\theta$ made by the director **n** with the layer normal ($z$ axis), we also have the **c** vector field, which represents the molecular projection on the smectic planes. In the presence of a magnetic field **H** at an angle $\alpha$ to the layer, in the $xz$ plane, we can construct a $2\pi$ splay or bend wall in the **c** vector field. The tilt director **n** is such that $n_x = \sin\theta\cos\phi$, $n_y = \sin\theta\sin\phi$, and $n_z = \cos\theta$. The free energy density for in plane distortions of **c** is given by

$$F = \frac{K}{2}(\phi_x)^2 - \frac{1}{2}\chi_a H^2[\sin\alpha\cos\theta + \cos\alpha\sin\theta\cos\phi]^2. \qquad (17)$$

Here we have ignored the coupling terms which naturally exist in $S_C$. The constant $K$ is the elastic constant associated with the distortion in the **c** vector field, and $\chi_a$ is the diamagnetic anisotropy. It must be remarked in this context that $F$ for an $S_C^*$ with the field along the layers was first worked out by Handschy and Clark [16]. This has been recently extended to $S_C$ in a tilted electric field [17]. We ignore $\theta$ variations in space and assume $\theta$ to be small. Minimization of the total energy with $\phi = \phi(x)$ leads to

$$K\phi_{xx} = \chi_a H^2[(\theta\sin\alpha\cos\alpha)\sin\phi + (\theta^2(\cos\alpha)^2)\sin\phi\cos\phi]. \qquad (18)$$

In recent times ferronematic (FN) systems have been experimentally realized in the laboratory [18–21]. A ferronematic is a normal nematic with magnetic grains suspended in them. The magnetization of all the grains are aligned in the same direction and along **n**. In view of the magnetization **M**, here also a $2\pi$ soliton is a natural topological object. In such systems, the free energy density for planar distortions in an external magnetic field is given by [22]

$$F = \frac{K}{2}(\phi_x)^2 - \frac{1}{2}\chi_a H^2(\cos\phi)^2 - MH\cos\phi \qquad (19)$$

where we have ignored grain segregation. Minimization in this case leads to

$$K\phi_{xx} = MH(\sin\phi) + \chi_a H^2(\sin\phi\cos\phi) \qquad (20)$$

which is similar to (18). Equation (18) or equivalently (20) is a double sine-Gordon equation which permits a $2\pi$ planar soliton solution in $\phi$ with most of the variation confined to a wall. Equations (18) and (20) have to be solved to get the respective soliton states. Each of these can be cast in the following form:

$$\phi_{xx} = A\sin\phi + B\sin\phi\cos\phi. \qquad (21)$$

The stability of a $2\pi$ soliton can be studied as a function of the ratio $(B/A)$. In both FN and $S_C$ we find that at $B = A$ the $2\pi$ soliton splits into two $\pi$ solitons. Interestingly in FN, after an initial split the separation monotonically slowly decreases, as shown in figure 5 ($a$) while in $S_C$ it monotonically increases as shown in figure 5 ($b$), with increasing values of $(B/A)$. Very similar effects can be expected in the case of a $2\pi$ twist soliton also. It must be remarked that in the case of FN we cannot go to very high fields in view of the grain migration at high $B/A$ ratio.

### 4.2. *Effects of elastic anisotropy*

We now consider the effects of splay–bend elastic anisotropy on the stability of a $2\pi$ splay or a $2\pi$ bend soliton. The equation of equilibrium in the presence of

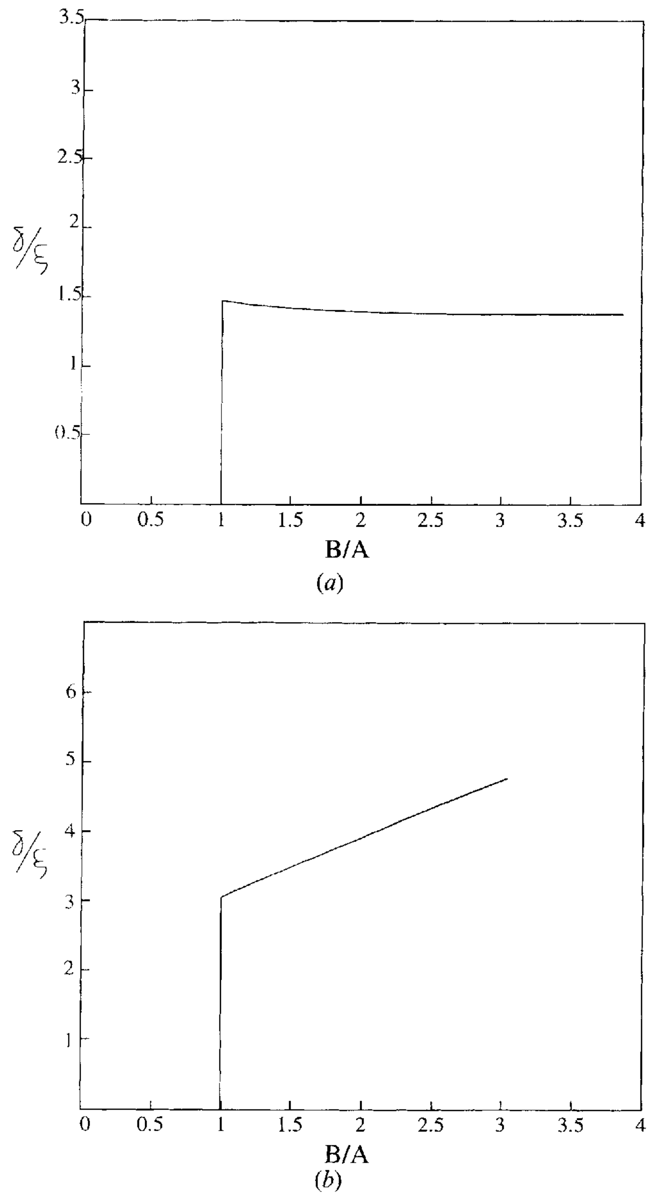


Figure 5. The separation between the two split $\pi$ solitons due to the instability of a $2\pi$ soliton ($a$) for ferronematics [$M = 0{\cdot}001$ G; $\chi_a = 10^{-6}$ cgs] ($b$) for $S_C$ in a tilted field with tilt angle $\alpha = 20°$ and the molecular tilt $\theta = 12°$. Here $\delta = \Delta - \Delta_0$, where $\Delta$ is the distance between the points at which the director is perpendicular to the field and $\Delta_0$ is the value of $\Delta$ for an unsplit $2\pi$ soliton.

elastic anisotropy is given by

$$\phi_{xx} = \frac{\sin(2\phi)}{(1-\varepsilon\cos(2\phi))}\left[\varepsilon(\phi_x)^2 + \frac{B}{2K_m}\right] + \frac{A\sin\phi}{(K_m)(1-\varepsilon\cos(2\phi))} \tag{22}$$

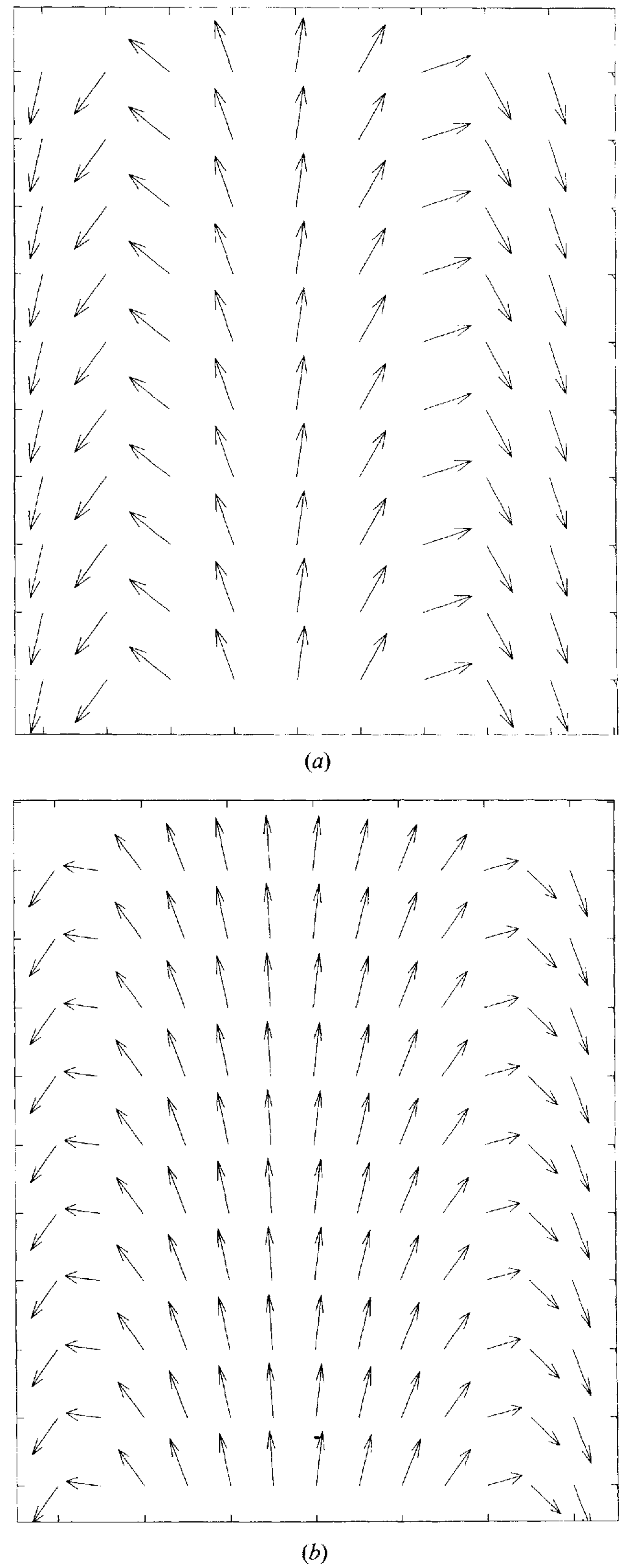


Figure 6. The director pattern associated with a $2\pi$ bend soliton ($a$) before split ($\varepsilon = 0$) and ($b$) after split due to elastic anisotropy ($\varepsilon \approx -0{\cdot}8$) [$K_{11} \approx 0{\cdot}2 \times 10^{-6}$ dynes, $K_{33} = 10^{-6}$ dynes and $H = 1000$ G].

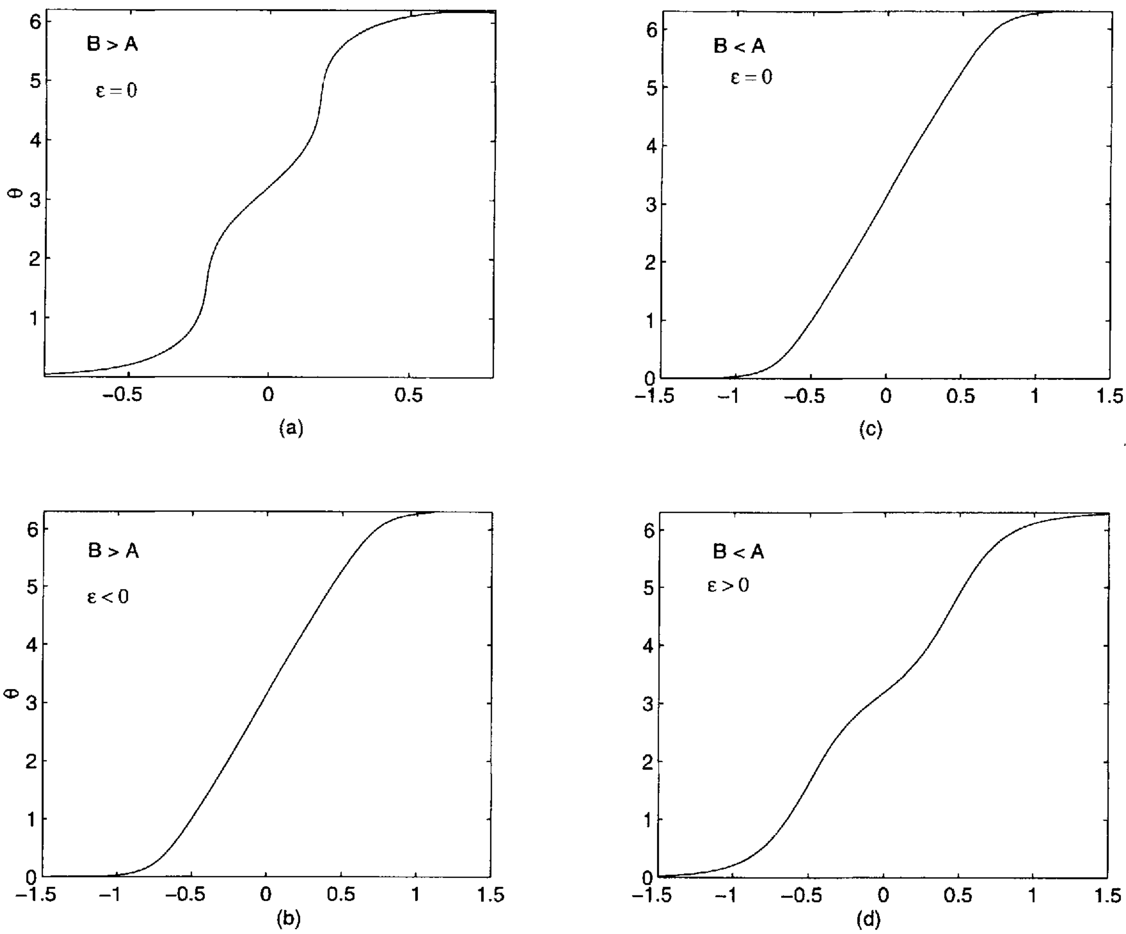


Figure 7. Effects of elastic anisotropy $\varepsilon$ and field on the structure of a $2\pi$ bend–splay soliton in a ferronematic or a $S_C$ in a tilted field. (*a*) and (*b*) represent the soliton profile with the same $B/A$, $(B/A > 1, [B/A = 10])$, but without and with an elastic anisotropy that annuls the split. (*c*) and (*d*) refer to a soliton with the same $B/A$, $(B/A < 1, [B/A = 0{\cdot}1])$ without and with elastic anisotropy. Here we see that the elastic anisotropy induces split. The abscissa is in units of $x/\xi$.



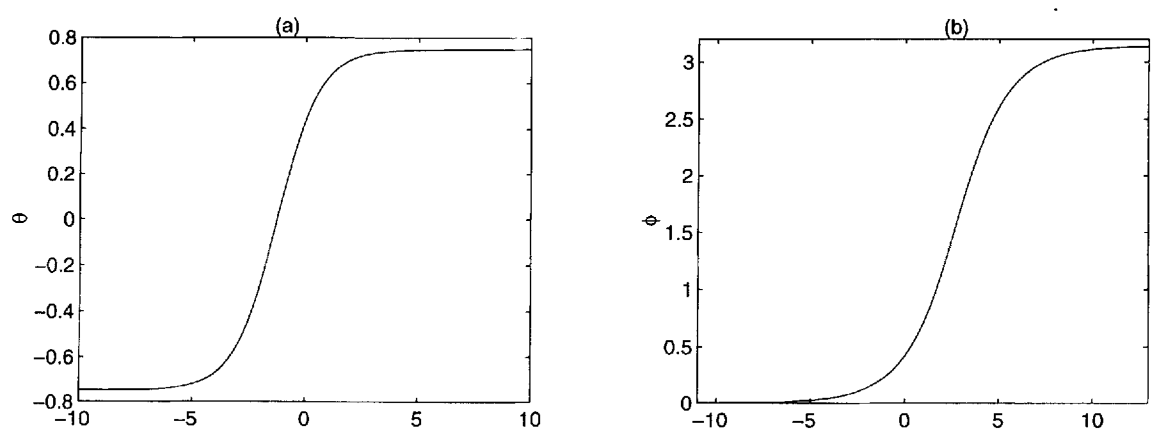


Figure 8. The orientation profile associated with (*a*) Ising wall and (*b*) ideal Bloch wall. The abscissa is in units of $x/\xi$. $[\theta_0 = 0{\cdot}76$, $H = 1000\,\mathrm{G}$, $K = 10^{-6}$ dynes and $\chi_a = 0{\cdot}1 \times 10^{-6}$ cgs].

where

$$\varepsilon = \frac{(K_{11} - K_{33})}{(K_{11} + K_{33})}. \qquad (23)$$

$K_{11}$ = splay elastic constant, $K_{33}$ = bend elastic constant and $K_m = (K_{11} + K_{33})/2$. We find that depending upon the sign of $\varepsilon$ a bend rich $2\pi$ soliton splits into two bend rich $\pi$ solitons or a splay rich $2\pi$ soliton splits into two splay rich $\pi$ solitons. The director pattern of a $2\pi$ bend soliton shown in figure 6 (*a*) before split ($\varepsilon = 0$) in 6 (*b*) after the split ($\varepsilon \neq 0$). Further, the split due to the field is either increased or decreased by the elastic anisotropy depending upon the sign of $\varepsilon$. In figure 7 we show these effects.

## 5. Structure of $\pi$ solitons in smectics

In previous discussion of $S_C$ we ignored spatial variations in $\theta$. However, near an $S_A$–$S_C$ phase transition we have to include gradients in $\theta$ in addition to the Landau terms $(a/2)\theta^2$ and $(b/4)\theta^4$. This has been done for a $\pi$ soliton that is permitted in a field parallel to the layers.

### 5.1. *Smectic C*

In a magnetic field parallel to the smectic planes, $+\mathbf{c}$ and $-\mathbf{c}$ states which are along and opposite to $\mathbf{H}$ are equivalent energetically. These two states can be connected in two different ways. In one case, they get connected through a gradual variation of the tilt angle $\theta$, from $-\theta_0$ to $+\theta_0$. Then it is like an Ising wall since the order parameter $\theta$ alone changes, vanishing at the centre of the wall. There is no $\mathbf{c}$ director distortion i.e. no $\phi$ variations associated with such a wall. In the other case, a $\pi$ bend or $\pi$ splay soliton connects $+\mathbf{c}$ and $-\mathbf{c}$ through a gradual variation in $\phi$ from 0 to $\pi$. This is akin to a Bloch wall. Here we discuss the structure of these walls.

#### 5.1.1. *Ising wall*

The free energy density in this case is

$$F = \frac{K}{2}(\theta_x)^2 + \frac{a}{2}(\theta)^2 + \frac{b}{4}(\theta)^4 - \frac{1}{2}\chi_a H^2(\theta)^2. \qquad (24)$$

In the $S_C$ phase $a < 0$ and $b$ is a small positive constant. The equation of equilibrium is

$$K\theta_{xx} = \theta(a - \chi_a H^2) + \theta^3 b. \qquad (25)$$

In figure 8 (*a*), we show $\theta$ variation present in such a wall with $\theta$ going from $-\theta_0$ to $+\theta_0$.

#### 5.1.2. *Bloch wall*

The free energy density in this case involves both $\theta$ and $\phi$ variations,

$$F = \frac{K}{2}(\theta_x)^2 + \frac{a}{2}(\theta)^2 + \frac{k}{2}\theta^2(\phi_x)^2 + \frac{b}{4}(\theta)^4 - \frac{1}{2}\chi_a H^2(\theta)^2(\cos\phi)^2. \qquad (26)$$

Minimization leads to

$$K\theta_{xx} = \theta[a - (\chi_a H^2(\cos\phi)^2) + (\phi_x)^2] + \theta^3 b \qquad (27)$$

and

$$K\phi_{xx} = \chi_a H^2 \sin\phi\cos\phi - \frac{2K}{\theta}(\theta_x)(\phi_x). \qquad (28)$$

Equations (27) and (28) have been numerically solved. We first consider an Ideal Bloch wall with $\phi$ variation only. This, however, is not a permitted solution of

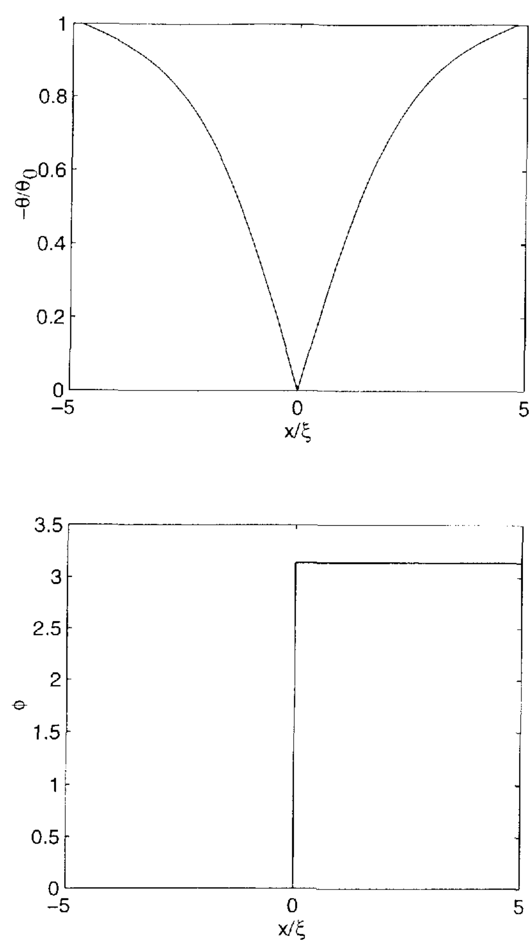


Figure 9. $\theta$ and $\phi$ profiles associated with a real $\pi$ Bloch wall where $\theta_0$ is the tilt angle at $x = \pm\infty$, [$\theta_0 = 1{\cdot}24$, $H = 1000\,$G, $K = 10^{-6}\,$dynes, $\chi_a = 10^{-6}\,$cgs and $a = -0{\cdot}14$].

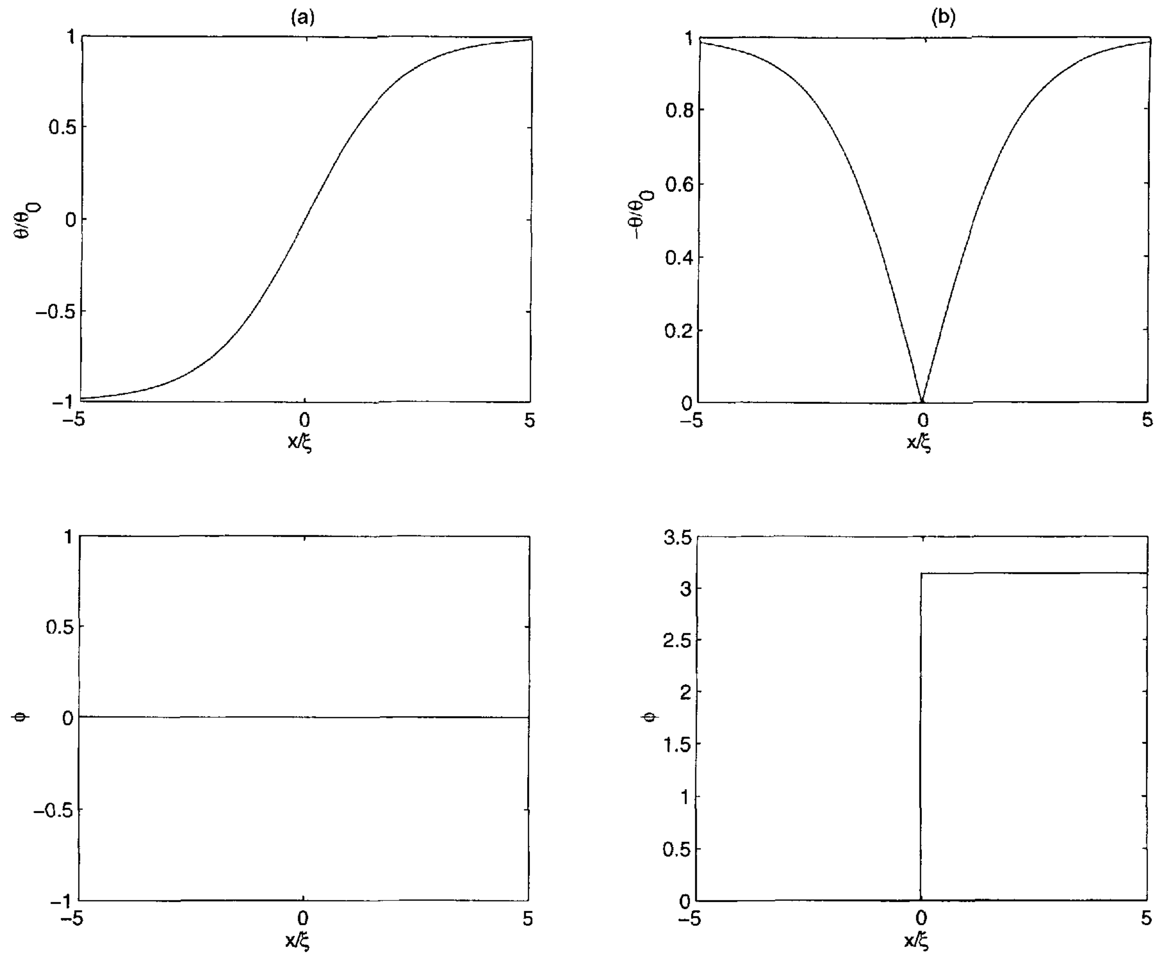


Figure 10. $\theta$ and $\phi$ profiles of an (*a*) Ising wall and (*b*) Bloch wall in $S_A$. The abscissa is in units of $x/\xi$. [$\theta_0 \approx 0{\cdot}68$, $H = 1000\,\mathrm{G}$, $K = 10^{-6}$ dynes, $\chi_a = 0{\cdot}1 \times 10^{-6}$ cgs and $a = 0{\cdot}54$].



equations (27) and (28). Its $\phi$ profile is shown in figure 8 (*b*). In figure 9 we give the variations in $\phi$ and $\theta$ associated with a real $\pi$ Bloch wall which is a solution of (27) and (28). It must be remarked that the width of an ideal Bloch wall is much greater than the width of the real Bloch wall in which $\theta$ and $\phi$ are coupled. In fact at high fields the width of a real Bloch wall is so narrow that it is not possible to distinguish it from the Ising wall since $+\theta$ with $\phi = 0$ is equivalent to $-\theta$ with $\phi = \pi$. However at low fields we get a Bloch wall of considerable width and it is structurally distinguishable from the Ising wall.

### 5.2. *Smectic A*

On the smectic A side of the $S_A$–$S_C$ phase transition, the coefficient $a$ is positive and $\theta$ is zero. Hence only above a threshold field $H_c = (a/\chi_a)^{1/2}$, we get a finite $\theta$. In this field induced tilt state we can construct an Ising or a Bloch soliton as in $S_C$. The $\theta$ and $\phi$ profiles for such walls are shown in figure 10. In this case Ising and Bloch walls become identical at all fields. It is to be noticed that at the centre of both Ising and Bloch walls $\theta$ vanishes. This is not contrary to intuition since at this point the magnetic contribution to $F$ vanishes and $a$ is positive implying $\theta$ to vanish. In principle differential equations (27) and (28) can also permit solutions where the $\theta$ does not vanish at the centre of the wall and $\phi$ going from 0 to $\pi$. But these solutions do not exhibit all the essential features of the soliton†.

One other interesting feature of our calculations in both $S_C$ and $S_A$ is that $\theta$ varies monotonically as $x \to 0$. This is in contrast to what we find in $S_C$ where $\theta$ exhibits oscillations [9]. Further it must be emphasized that in all the above cases the smectic layer undulations induced by the field can be neglected since in thick samples, the wavelength of such instabilities is very large compared to its amplitude.

Similar situations arise in the case of $S_C$ in a tilted

† We thank Sreejith Sukumaran for discussions on this point.

field. Here also we can construct a $2\pi$ planar soliton. The $\theta, \phi$ profiles in these soliton structures are not very different from those found for $\pi$ solitons in a $H$ parallel to the layers.

## 6. Combination of solitons

In view of the fact different soliton states are permitted in a given geometry, we can think of their simultaneous existence or in other words, a smooth topological connection between the different solitons. This is a well-known process in normal nematics where planar solitons get connected by Bloch or Neel lines [23]. A similar exercise leads to some interesting situations in $S_C$ and $\chi_a < 0$ nematics.

In the previous section we found that $+\mathbf{c}$ and $-\mathbf{c}$ states can be connected through either a Bloch wall or an Ising wall. It is therefore possible that in a narrow range of parameters, these walls have comparable energies. Therefore we postulate, the possible existence of a line disclination connecting these two topological walls.

In $\chi_a > 0$ or $\varepsilon_a > 0$ nematics, obtained from an unwinding of a cholesteric, we have two solitons namely the bend soliton and the twist or the anti-twist soliton connecting the same base states. From the discussions presented in § 3, we find that the ATS and a bend soliton can sometimes have comparable energies. Therefore we can think of a $\lambda$ line [23] connecting these two planar solitons.

In normal $\chi_a < 0$ nematics, though $\lambda$ lines do not exist we can construct objects combining a planar soliton with a radial soliton. From figures 1 (*a*) and 2 (*c*) we see that in both the splay–bend radial soliton and the splay planar soliton the degenerate base states are perpendicular to the field **H** at large distances. Hence we can think of a combination of these structures as shown in figure 11. Here one half of the pattern represents a planar splay soliton which gets smoothly connected to half of a radial splay-bend soliton. In a similar way, we can also combine a twist planar soliton with a bend twist circular soliton.

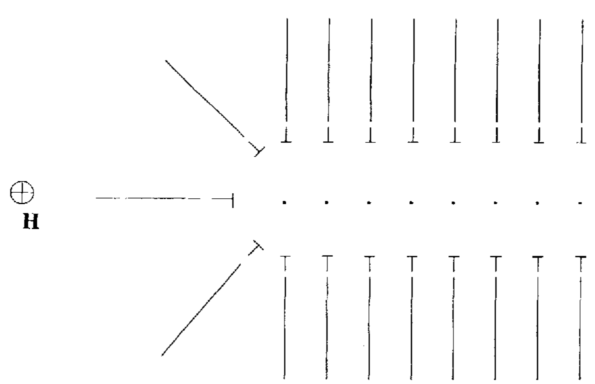


Figure 11. Combination of a splay–bend radial soliton with a splay–bend planar soliton. At the centre the director **n** is along **H** which is perpendicular to the plane of the figure. The nail heads indicate that the director **n** is tilted out of the plane of the figure.

Finally we consider an unwound cholesteric with $\chi_a < 0$. We may be tempted to construct an intertwined soliton in this nematic. However calculations show that the $\theta$ profile is not a soliton. The $\theta$ and $\phi$ profiles are like those of a $\pi$ soliton in $S_C$ which was discussed earlier.

## 7. Conclusions

We find intertwined planar solitons as possible defect states in nematics. They are walls with out of plane distortions associated with them. In unwound cholesterics and nematics with high dielectric anisotropy, we have worked out the energetics of bend and twist solitons which connect the same base states. The problem of the elastic stability of a $2\pi$ bend or splay soliton in $S_C$ and FN due to a field and elastic anisotropy has been considered. We have also worked out the structure of a $\pi$ soliton in $S_A$ and $S_C$ phases near an $S_A$–$S_C$ phase transition.

Our thanks are due to K. A. Suresh and Sreejith Sukumaran for helpful comments.

## References

[1] Volovik, G. E., and Mineev, V. P., 1976, *Soviet Phys. JETP Lett.*, **24**, 561.
[2] Lam, L., 1991, *Solitons in Liquid Crystals*, edited by L. Lam and J. Prost (Springer-Verlag, New York), p 11.
[3] Helfrich, W., 1968, *Phys. Rev. Lett.*, **21**, 1518.
[4] De Gennes, P. G., 1971, *J. Phys. (Paris)*, **32**, 789.
[5] Leger, L., 1972, *Solid State Commun.*, **11**, 1499.
[6] Leger, L., 1973, *Mol. Cryst. liq. Cryst.*, **24**, 33.
[7] Brochard, F., 1973, *Mol. Cryst. liq. Cryst.*, **23**, 51.
[8] Pindak, R., Young, C. Y., Meyer, R. B., and Clark, N. A., 1980, *Phys. Rev. Lett.*, **45**, 1193.
[9] Yamashita, M., 1985, *Prog. Theor. Phys.*, **74**, 622.
[10] Babylev, Y. B., and Pikin, S. A., 1977, *Soviet Phys. JETP.*, **45**, 195.
[11] Yamashita, M., 1984, *J. phys. Soc. Jpn.*, **53**, 1097.
[12] De Gennes, P. G., 1968, *Solid State Commun.*, **6**, 163.
[13] Meyer, R. B., 1968, *Appl. Phys. Lett.*, **12**, 281.
[14] Hudak, O., 1983, *J. Phys.*, **44**, 57.
[15] Sunil Kumar, P. B., and Ranganath, G. S., 1991, *Mol. Cryst. liq. Cryst.*, **196**, 27.
[16] Handschy, M. A., and Clark, N. A., 1984, *Ferroelectrics*, **59**, 69.
[17] Stewart, I. W., Carlsson, T., and Leslie, F. M., 1994, *Phys. Rev. E*, **49**, 2130.
[18] Rault, J., Cladis, P. E., and Burger, J. P., 1970, *Phys. Lett.*, **32A**, 199.
[19] Hayes, C. F., 1976, *Mol. Cryst. liq. Cryst.*, **36**, 245.
[20] Chen, S. H., and Amer, N. M., 1983, *Phys. Rev. Lett.*, **51**, 2298.
[21] Chen, S. H., and Chiang, S. H., 1987, *Mol. Cryst. liq. Cryst.*, **144**, 359.
[22] Sunil Kumar, P. B., and Ranganath, G. S., 1993, *J. Phys. II France.*, **3**, 1497.
[23] Ranganath, G. S., 1987, *Mol. Cryst. liq. Cryst.*, **154**, 43.